HEFAT2012
9th International Conference on Heat Transfer, Fluid Mechanics and Thermodynamics
16 – 18 July 2012
Malta

VOID FRACTION MEASUREMENTS OF REFRIGERANT FLOW IN SMALL DIAMETER TUBES USING A CAPACITIVE SENSOR

De Kerpel K.* and De Paepe M.
*Author for correspondence
Department of Flow Heat and Combustion Mechanics,
Ghent University- UGent,
Ghent, 9000,
Belgium,
E-mail: Kathleen.DeKerpel@UGent.be

ABSTRACT

The void fraction is one of the key parameters in two phase flows. Quite a few methods have been proposed to measure this void fraction. Yet many of these methods are quite complex, intrusive and/or are not applicable to all possible void fraction ranges. Capacitance measurements have already been shown to characterize the two phase flow behaviour of refrigerants. Due to the curvature of the electrodes for circular tubes, the measured capacitance does not vary linearly with the void fraction. In this work a method is proposed to calibrate a capacitive sensor and thus determine the void fraction based on capacitive measurements. The proposed method was applied to 270 measurement points. The tube diameter D for all these points is 8mm, the mass flux ranges from 200 to 500 kg/m²s and the vapour fraction ranges between 2.5% and 97.5%. Refrigerants R134a and R410A were used. The results for these data points were compared to the Rouhani-Axelsson drift flux void fraction model. A very good agreement with this model was observed.

INTRODUCTION

Quite a number of experimental methods have already been proposed to measure the void fraction of two phase flow. Yet, most of these methods are either intrusive (such as the conductive methods), not widely applicable (the optical methods) or very complex and expensive (e.g. gamma or neutron attenuation).

In optical methods, visual images of the flow are processed to determine the void fraction. This requires a transparent tube (glass or plastic) which limits the possible temperatures and pressures. Ursenbacher et al. [1] developed an optical technique to determine the void fraction which showed a good agreement with the drift flux void fraction model by Rouhani-Axelsson [2]. However, this optical method could only be used for stratified flow regimes, which limits the applicability of the measurement technique.

Methods based on X-ray attenuation, like the one applied by Owen et al. [3] do not require a transparent tube. Yet there are serious cost and safety issues connected to this method.

Ultrasonic transmission techniques detect changes in acoustic impedance which is closely related to the density of the media. However, a gas-liquid interface acts almost as a perfect mirror for an acoustic wave. This technique can therefore only be used for total void fractions up to 20%, [4].

Capacitive void fraction measurements are often used, because they are quite easy to implement, non intrusive and relatively low cost compared to some other techniques. For air-water flow and oil-water flow this has already been performed [5], [6] and [7]. Keska et al. [6] made a comparison of four techniques to measure the flow behaviour: a resistive method, a capacitive method, an optical method and a static pressure based method. It was concluded that the capacitive and resistive methods were both very effective to characterize the flow behaviour. Canière et al. [8] also showed that the measured time signal of a capacitance sensor can be used to characterize the flow regime of a refrigerant two phase flow. Yet the capacitive sensor used by Canière et al. [8] was uncalibrated, it provided a signal related to the capacitance, but not the actual void fraction value. In this work a calibration method for this sensor is proposed, so the void fraction can be measured.

CAPACITIVE SENSOR BY CANIÈRE ET AL.

The sensor designed by Canière te al. [8] was used in a straight round tube with an 8mm diameter. The sensor consists of two concave electrodes, both with an angle of 160° and a length of 8mm. For more information about the sensor construction we refer to [9], [10] and [11]. Due to the difference between the dielectric constant of the gas and liquid phase, the measured capacitance between the electrodes depends on the void fraction. However, due to the curvature of the electrodes the electric field is not homogeneous. As a result of this, the measured capacitance is dependent not only on the void fraction but also on the spatial distribution of the phases and the capacitance does not vary linearly with the void

fraction. In Figure 1 void fractions derived by assuming a linear variation of the measured capacitance between full vapour and full liquid flow are shown for R410A, T=15°C, G=200 kg/m²s and D=8mm. The void fraction predicted by the Rouhani–Axelsson drift flux void fraction model and the homogeneous void fraction model are also shown for comparison. The measured values do not agree with the Rouhani–Axelsson drift flux void fraction model, which has been shown to be one of the most accurate void fraction models for this kind of flow by both Thome et al. [12] and Ghajar et al. [13].

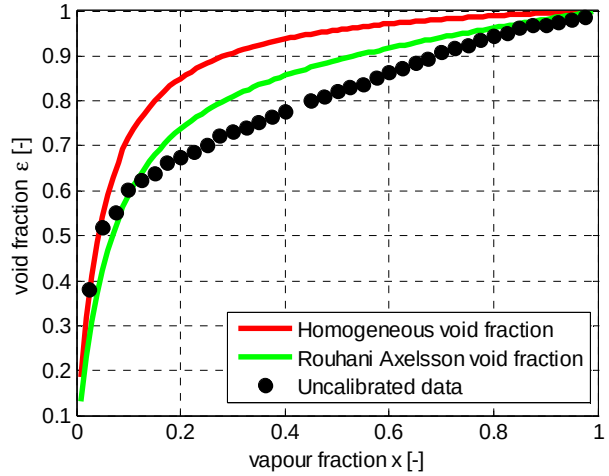

Figure 1 Void fraction data without calibration (linear C-ε relation assumed) for R410A, T=15°C, G=200 kg/m²s and D=8mm. The void fraction predicted by the Rouhani–Axelsson drift flux void fraction model and the homogeneous void fraction model are also shown for comparison

The sensor design can be modified to reduce the impact of the spatial distribution of the phases. This could be done by reducing the electrode angle, as shown by Strazza et al. [7] for a water-oil annular flow. However, the difference in dielectric constant between the phases is quite small for refrigerants, compared to that for water-oil flow. For R134a at 15°C the difference of the dielectric constant of the liquid phase to that of the gas phase is about 7, whereas for water-oil flow and air-water flow this is about 80. Because of the small difference in dielectric constant between the phases, the measured capacitance difference between total vapour flow (ε = 1) and total liquid flow (ε = 0) is in the order of 1pF for the sensor designed by Canière et al.[8]. Reducing the electrode angle or the electrode length will reduce the measured capacitance values even further, which will make it difficult to obtain measurements with a low uncertainty. As both the flow regime and the void fraction are important influence factors for the pressure drop and heat transfer, it would be convenient if they could be both determined using this capacitive sensor. To this end, the capacitive void fraction sensor designed by Canière et al. needs to be calibrated so that it is also able to measure the void fraction.

DATASET

Canière et al. [14] designed a test setup and recorded a large dataset for R134a and R410A at varying mass flux and vapour quality x. For each point in the dataset the temperature is 15°C and the inner tube diameter is 8mm. The capacitance sensor designed by Canière et al. was used to record signals at all points and these signals were analysed to be used as flow regime discriminator. A probabilistic unsupervised flow mapping technique was developed [9] and a flow regime was assigned to each point of the dataset. A three group classification was considered: slug, annular and intermittent flow. In Figure 2 the result of this flow regime classification is shown.

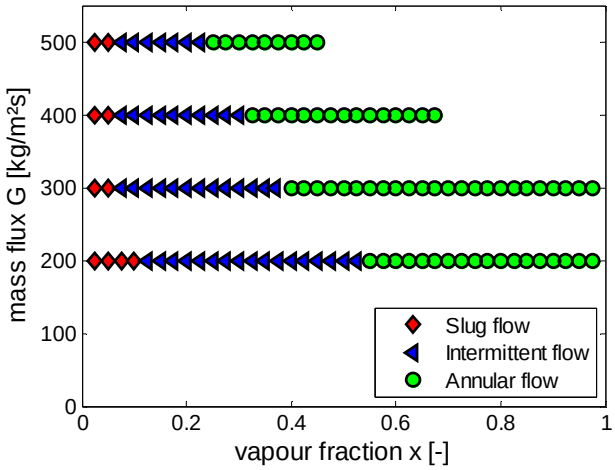

a) R134a, D=8mm and T = 15°C

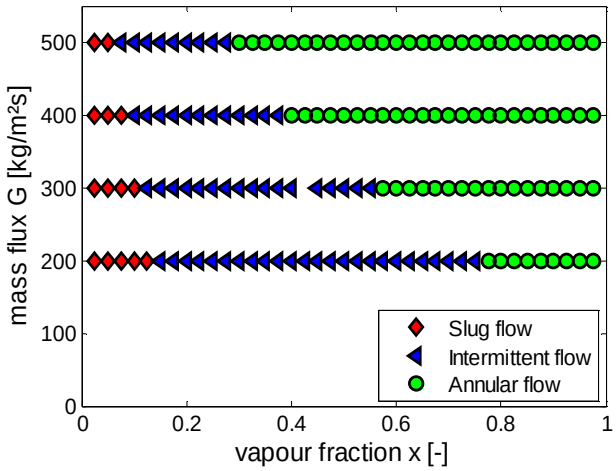

b) R410A, D=8mm and T=15°C

Figure 2 Results of the flow mapping technique by Canière et al. [9]

INTERFACE STRUCTURE FOR THE DIFFERENT FLOW REGIMES

In order to calibrate the capacitive sensor taking into account the spatial distribution of the phases, the possible spatial phase distributions need to be known. This distribution

depends on the flow regime. In the next section the assumed phase distribution is discussed for each of these flow regimes.

Slug Flow

For slug flow, the interface structure has a periodical variation. This is illustrated in Figure 3, showing the elongated gas bubbles (Figure 3 a)) which alternate with liquid slugs with just a few vapour bubbles in them (Figure 3b)).

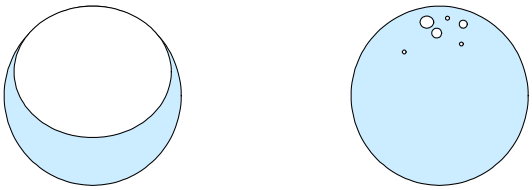

a) Simplified flow structure for elongated bubble

b) Simplified flow structure for liquid slug

Figure 3 Interface structures for slug flow (liquid phase is shown blue and vapour phase white)

For the elongated bubble flow structure, the shape of the elongated bubble is important to determine the calibration curve. In literature, very little was found about this subject. Two simple cases were compared: one where the liquid forms a stratified layer at the bottom of the tube and one where the vapour bubble is perfectly cylindrical. For the latter case the gas core is positioned in the tube so that it touches the tube wall at its highest point. The C-ε relation for these cases was determined using FEM simulations. The results are shown in Figure 4. Both these calibration curves were used to determine a void fraction for each slug measurement, the results were compared to the Rouhani–Axelsson drift flux void fraction model and the homogeneous void fraction model. The agreement with the Rouhani–Axelsson model for the cylindrical elongated bubble assumption was very good. This model was also shown to be the best prediction method for the average void fraction in horizontal straight tubes by Wojtan et al. [15] and Ghajar et al. [13]. In Figure 4 the normalized C-ε relation is shown, this is calculated as:

$$C_{norm} = \frac{C - C_{vapour}}{C_{liquid} - C_{vapour}} \qquad (1)$$

For the stratified bubble assumption the void fraction was systematically overestimated. Moreover, in more than 50% of the cases, the calculated void fraction for this assumption was larger than the homogeneous void fraction, which is not possible [16].

For the liquid slug, the flow structure is mainly all liquid flow with just a few small vapour bubbles which are mostly quite close to the top wall of the tube. This can be seen in Figure 3b). For this flow structure, the cylindrical vapour bubble assumption also gave good results. For other (not spherical) vapour bubble geometries the results were only marginally different from that for spherical ones. Hence, the C-ε relation for cylindrical vapour bubbles can be used for determining the void fraction for both the elongated vapour bubbles as for the liquid slugs. The results of the calibration are shown in the next paragraph.

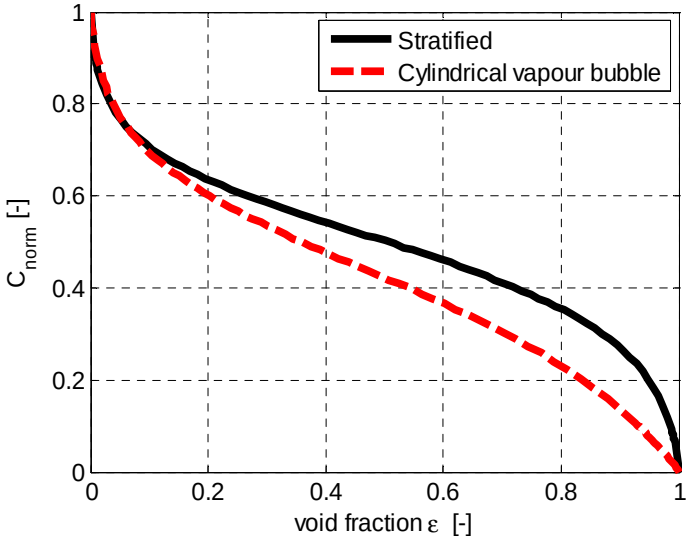

a) Normalized C-ε relation for stratified and cylindrical vapour bubbles

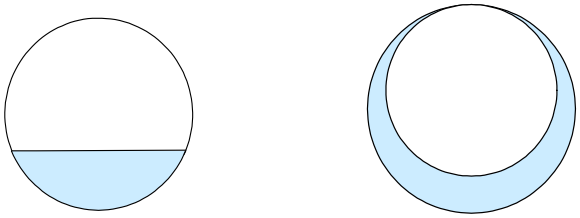

b) Stratified vapour bubbles

c) Cylindrical vapour bubbles

Figure 4 Results of FEM simulations for slug flow with stratified and with cylindrical elongated vapour bubbles. The assumed flow structures are also shown (liquid phase is shown blue and vapour phase white)

Intermittent flow

The interface structures for slug and annular flow are quite different from one another. The intermittent flow regime can be seen as a transitional flow regime between slug flow and annular flow. For a low vapour quality x, it shows a lot of similarity with slug flow. Liquid waves obstructing a large part of the tube cross section still occur, though they don't reach the top of the tube anymore. For higher x, the flow behaviour starts to look more and more like annular behaviour.

Because the intermittent flow structure seems to be a transition between slug and annular flow and because there was very little literature found about structure of intermittent flow, the void fraction for this flow regime is determined as a weighted average of the void fraction for slug flow and that for annular flow. The weighing is based on the vapour fraction x as shown in equation (2):

$$\varepsilon_{\text{int ermittent}} = \frac{(x - x_{IS})}{(x_{IA} - x_{IS})}\varepsilon_{annular} + \frac{(x_{IA} - x)}{(x_{IA} - x_{IS})}\varepsilon_{slug} \qquad (2)$$

In this equation x_{IS} is the vapour fraction at which the slug-intermittent flow transition occurs and x_{IA} is the vapour fraction at which the intermittent-annular transition occurs. Two methods to determine x_{IS} and x_{IA} were tested and gave relatively good results:

- **Method 1:** x_{IS} and x_{IA} are determined from experimental results. For the expected G and x range a certain amount of measurement points need to be available. For each measurement from this dataset the flow regime is determined using the method by Canière et al. [9] and a flow map for the measured data can be plotted. From this flowmap x_{IS} and x_{IA} can then be determined.
- **Method 2:** x_{IS} and x_{IA} are determined using a flowmap. Two different flow maps were tested for this method: the Wojtan-Ursenbacher-Thome flow map [17] and the intermittent-annular transition boundary by Barbieri et al. [18] combined with the slug-intermittent transition boundary of the Wojtan-Ursenbacher-Thome flow map. [14] had previously found that this last combination best agreed with the recorded dataset.

Annular Flow

Figure 5 a) shows the simplified structure for annular flow: a liquid ring with a vapour core in the middle. Yet, this is not a very realistic flow structure. In the vapour core, liquid droplets of various sizes can be entrained. Also, for horizontal tubes the liquid film tends to be thicker at the bottom of the tube due to gravity. A more realistic (though exaggerated) annular flow structure is shown in Figure 5b).

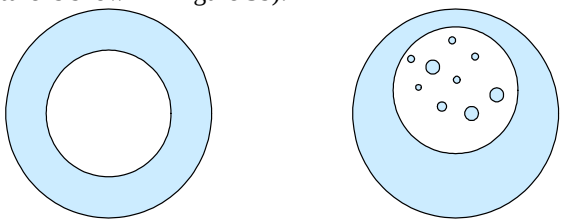

a) simplified b) realistic

Figure 5 Annular flow liquid-vapour interface structure (liquid phase is shown in blue and vapour phase white)

It goes without saying that to perform an adequate calibration; a realistic flow structure should be assumed when determining the C-ε curve. Yet, this is only necessary if the C-ε relation for the realistic flow structure differs significantly from that for a simplified flow structure.

The effect of gravity on the annular flow structure can be expressed as the asymmetry of the liquid film; this is defined as the ratio of the liquid film thickness at the bottom δ_{bottom} and the liquid film thickness at the top δ_{top}. In Figure 6 the asymmetry of the liquid film is shown as calculated with the correlation of Schubring et al. [19]. Comparing this to the data shown in Figure 2 one can clearly see that the asymmetry is always lower than 3 for a G and x where the flow regime is annular. The results for R410A are not shown here, but for this case the asymmetry is also limited to 3.

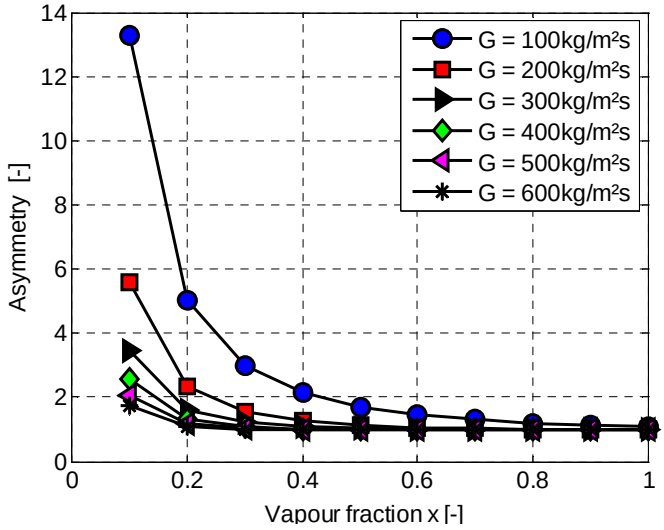

Figure 6 Asymmetry of the annular liquid film for R134a, T = 15°C and D=8mm

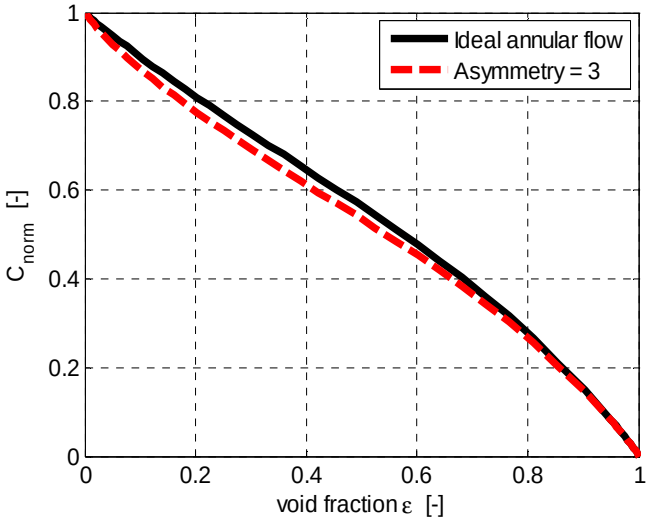

Figure 7 effect of liquid film asymmetry on the normalized calibration curve for R134a

In Figure 7 the effect of the assymetry of the liquid film on the normalized calibration curve is shown. For annular flow the void fraction is typically large, in Figure 11 and Figure 12 furtheron it can be observed that the minimum void fraction for annular flow is 80%. For these high void fractions the effect of the assymetry of the film is small to negligible.

Next, the correlation of Oliemans [20] is used to determine the entrained fraction. The entrained fraction *e* is defined as the ratio of the mass flow rate of droplets in the gas core m_{drop} to the total liquid mass flow rate m_{liq}. The maximum droplet hold up γ can now be estimated by neglecting the slip between the gas phase and the liquid droplets [21], thus assuming they are

small enough to follow the gas flow rather than suffer from their inertia:

$$\gamma = e\frac{\varepsilon}{1-\varepsilon}\frac{1-x}{x}\frac{\rho_g}{\rho_l} \qquad (3)$$

In equation (3) the void fraction ε is determined with the Rouhani–Axelsson drift flux void fraction model. Figure 8 shows the predicted droplet hold up for R134a at 15°C, one can see that γ is limited to 0.2 for all mass fluxes. For the sake of simplicity, the droplet hold up for other temperatures and for R410A is not shown here, though they are all limited to 0.2.

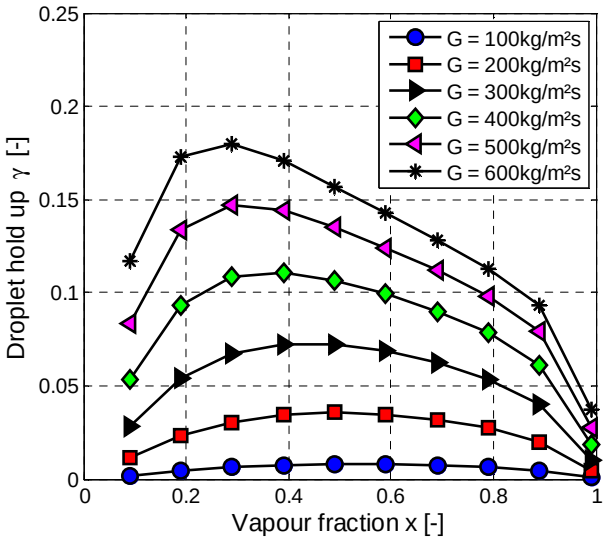

Figure 8 droplet hold up γ in the gascore for R134a, T=15°C and D=8mm

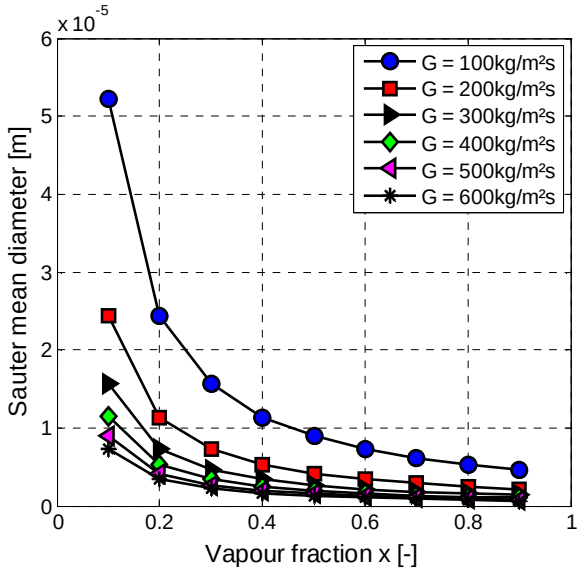

Figure 9 Sauter mean diameter of the entrained droplets for R134a calculated with the correlation of Azzopardi [22]

The Sauter mean diameter of the entrained droplets can be determined with the correlation of Azzopardi [23] the results for R134a are shown in Figure 9. One can see that the Sauter mean diameter of the droplets is mostly in the order of 10µm. For low vapour fractions the Sauter mean diameter is larger, but for these conditions the flow is not annular (see Figure 2). The results for R410A are not shown here for simplicity, but they are entirely similar. As a result for both refrigerants, the sauter mean diameter of the entrained droplets for annular conditions does not seem to be influenced much by G or x.

Yet, the droplet hold up γ does vary quite a lot with G and x. If the effect of the entrained droplets would be accounted for in the calibration curves, this would make the calibration quite dependent of G, x and the correlations that are used to predict the entrained fraction. Therefore, as a first approximation, the annular interface is assumed to be a perfect circular ring structure as depicted in Figure 5a), without considering the entrainment.

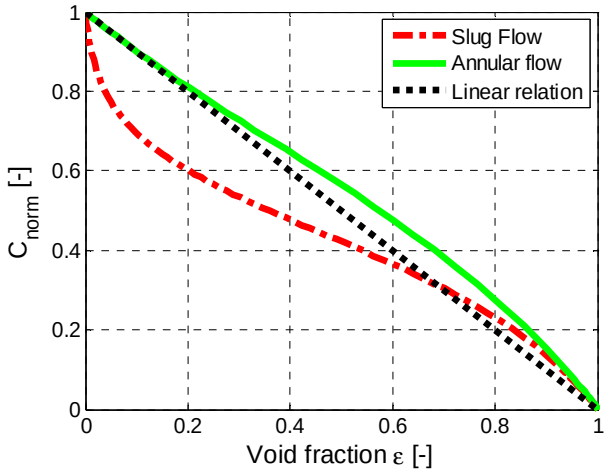

a) R134a

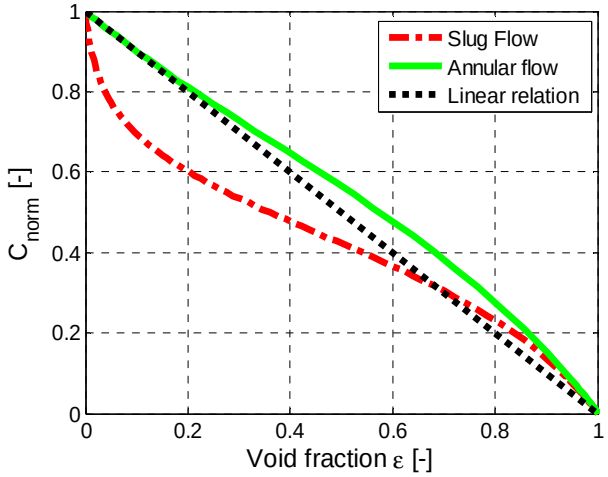

b) R410A

Figure 10 Normalized C-ε relation for R134a and R410A, the linear relation was used for the uncalibrated data

As will be discussed further on, this approximation yields quite good results for the low mass fluxes, where the droplet hold up is limited. For higher mass fluxes the approximation leads to a slight over estimation of the void fraction. These results are shown in the next paragraph.

RESULTS AND DISCUSSION

The calibration curves for R410A and R134a which are the result of the assumed interface structures as discussed in the previous paragraph are shown in Figure 10.

The results of the calibration are shown in Figure 11 for R134a and in Figure 12 for R410A. For these figures x_{IS} and x_{IA} are determined from measurements (method 1). The results for the other weighing methods are not shown here, but they are compared in Table 1. It is observed that each method gives a quite similar result. The actual choice of the method to use can therefore mainly depend on practical considerations.

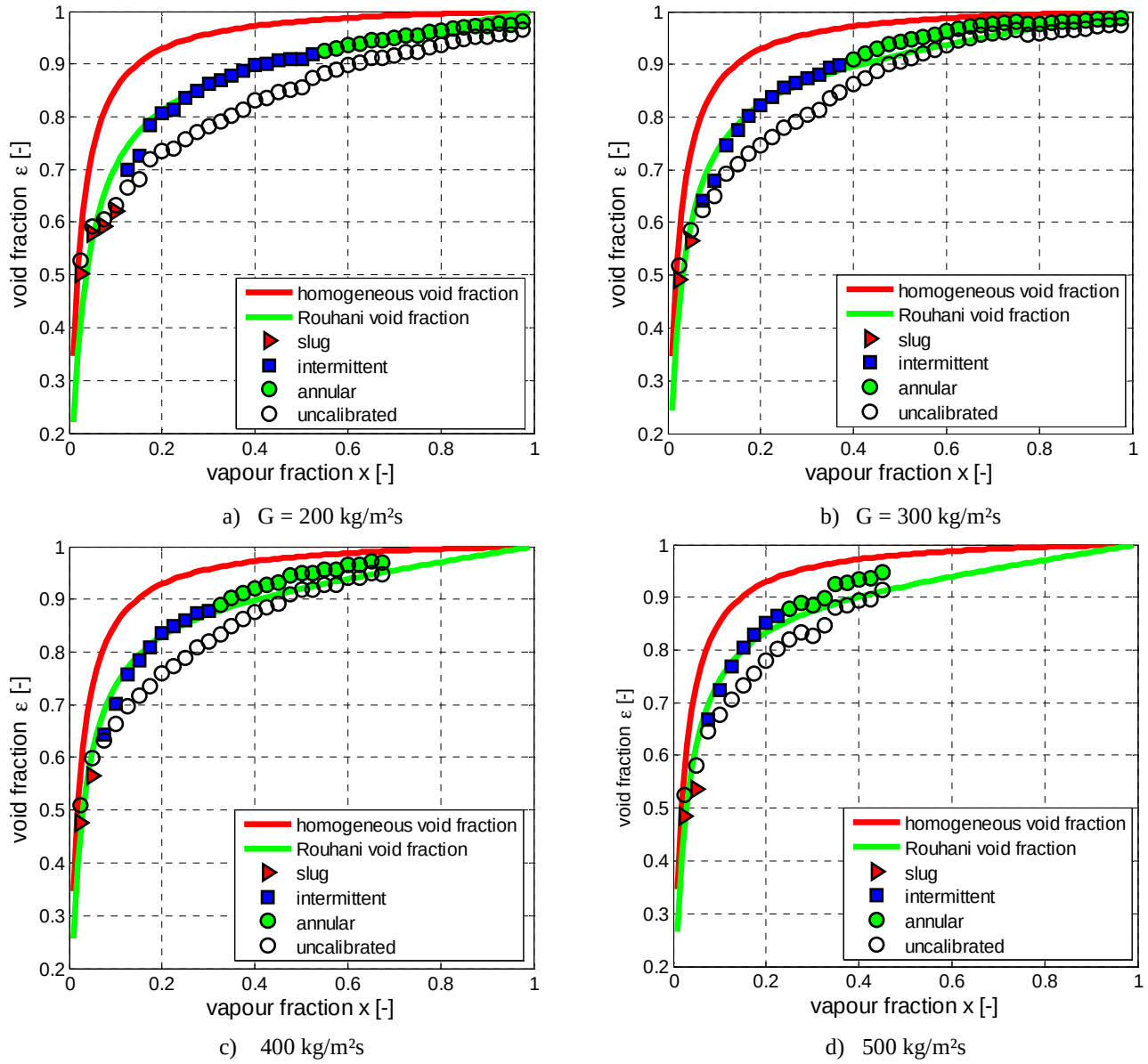

Figure 11 calibration results for R134a, the weighing for intermittent flow is based on the vapour fraction, x_{IS} and x_{IA} are determined from measurements. For the uncalibrated measurements, a linear C-ε relation is assumed.

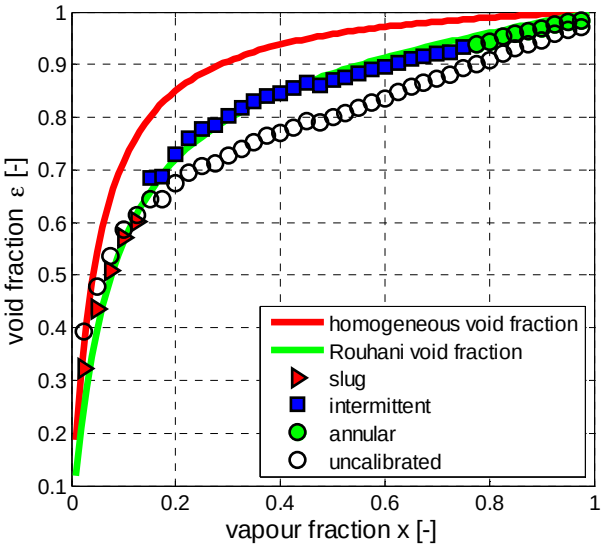

a) G = 200 kg/m²s

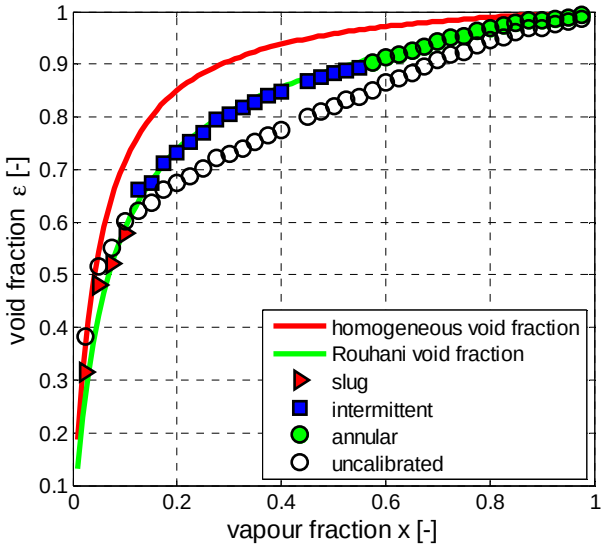

b) G = 300 kg/m²s

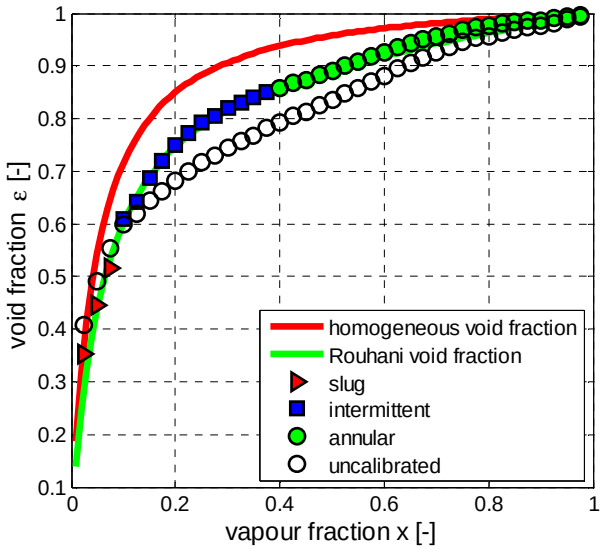

d) G = 400 kg/m²s

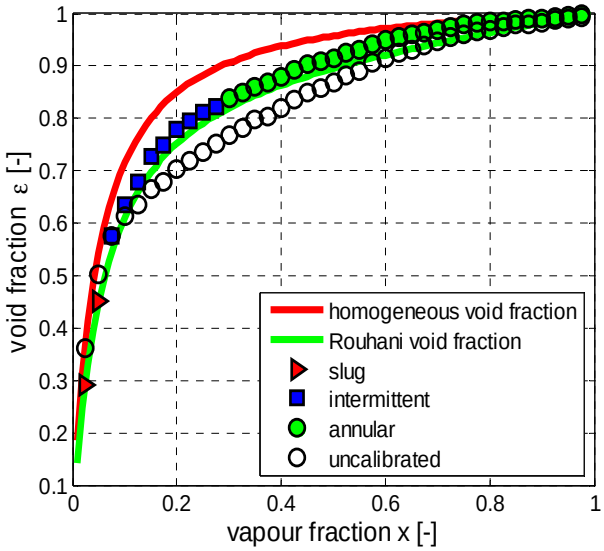

c) G = 500 kg/m²s

Figure 12 calibration results for R410A, the weighing for intermittent flow is based on the vapour fraction, x_{IS} and x_{IA} are determined from measurements. For the uncalibrated measurements, a linear C-ε relation is assumed

	method 1		method 2			
			Thome flowmap		Barbieri flowmap	
	μ (%)	σ (%)	μ (%)	σ (%)	μ (%)	σ (%)
R410A, Slug Flow	4,514	10,227	1,7492	10,68	1,7492	10,68
R410A, Intermittent flow	0,224	1,804	2,0793	3,5878	2,0824	4,3032
R410A, Annular flow	0,806	1,260	0,2731	1,6120	0,5477	1,4775
R410A, Total	0,905	3,508	1,0652	4,6661	1,1539	4.7400
R134a, Slug Flow	-2,356	12,253	-3,6619	9,3178	-3,6619	9,3178
R134a, Intermittent flow	-0,8266	2,381	0,4864	1,8933	-0,297	1,2539
R134a, Annular flow	1,332	1,332	1,218	1,5783	1,3919	1,4756
R134a, Total	0,19	4,02	0,1529	4,4432	0,1171	4,397

Table 1 comparison of the different weighing methods to the Rouhani–Axelsson drift flux void fraction model. Method 1: x-based weighing, x_{IS} and x_{IA} are determined from measurements. Method 2: x-based weighing, x_{IS} and x_{IA} are determined from flowmaps.

Figure 11 and Figure 12 show the results for the time averaged void fraction. However, the void fraction varies in time. This is very pronounced for slug flow and intermittent flow. The Rouhani–Axelsson drift flux void fraction model might predict the average void fraction very well; it cannot predict the dynamic behaviour of the void fraction. This can be measured using the capacitive void fraction sensor designed by Canière et al. combined with the proposed method.

CONCLUSIONS

A method to calibrate the capacitive sensor designed by Canière et al. [14] was proposed. For this method, a separate C-ε relation is used for each flow regime, to account for the sensitivity of the sensor to the spatial distribution of the phases. For slug and annular flow, the used C-ε relation is found with FEM simulations.

For intermittent flow a weighing between slug and annular flow is proposed. Two different weighing methods were compared to the Rouhani–Axelsson drift flux void fraction model. This model was shown by different authors ([13] and [15]) to give the best prediction of the time averaged void fraction. Both methods gave comparably good agreement with the Rouhani-Axelsson correlation. The weighing method to be used can therefore be selected on practical considerations, which makes this method widely applicable.

NOMENCLATURE

G	[kg/m²s]	Mass flux
C	[F]	Capacitance
C_{liquid}	[F]	Capacitance for all liquid flow
C_{norm}	[-]	Normalized capacitance
C_{vapour}	[F]	Capacitance for all vapour flow
e	[-]	entrained fraction of liquid in the annular gas core
m_{drop}	[kg/s]	mass flow rate of droplets entrained in the annular gas core
m_{liq}	[kg/s]	total liquid mass flow rate
x	[-]	vapour fraction
x_{IA}	[-]	vapour fraction at which the intermittent-annular transition takes place
x_{IS}	[-]	vapour fraction at which the slug-intermittent transition takes place

Special characters

γ	[-]	droplet hold up in the annular gas core
ε	[-]	void fraction
$\varepsilon_{annular}$	[-]	void fraction determined with C-ε relation for annular flow
$\varepsilon_{intermittent}$	[-]	void fraction determined with C-ε relation for intermittent flow
ε_{liquid}	[-]	dielectric constant of the liquid phase
ε_r	[-]	dielectric constant
ε_{slug}	[-]	void fraction determined with C-ε relation for slug flow
ε_{vapour}	[-]	dielectric constant of the vapour phase
μ	[-]	mean
ρ_g	[kg/m³]	density of the gas phase
ρ_l	[kg/m³]	density of the liquid phase
σ	[-]	standard deviation

ACKNOWLEDGMENTS

This research was funded by a Ph.D. grant of the Agency for Innovation by Science and Technology (IWT).

REFERENCES

[1] Ursenbacher T., Wojtan L. and Thome J. R., Interfacial measurements in stratified types of flow. Part I: New optical measurement technique and dry angle measurements, *International Journal of Multiphase Flow*, Vol. 30, 2004, pp. 107-124

[2] Rouhani S. Z. and Axelsson E., Calculation of Void Volume Fraction in Subcooled and Quality Boiling Regions, *International Journal of Heat and Mass Transfer*, Vol. 13, 1970, pp. 383-393

[3] Owen C., Jones J. and Zuber N., The interrelation between void fraction fluctuations and flow patterns in two-phase flow, *International Journal of Multiphase Flow*, Vol. 2, 1975, pp. 273–306

[4] Rahim R. A., Rahiman M. H. F., Chan K. S. and Nawawi S. W., Non-invasive imaging of liquid/gas flow using ultrasonic transmission-mode tomography, *Sensors and Actuators a-Physical*, Vol. 135, 2007, pp. 337-345

[5] Abouelwafa M. S. A. and Kendall E. J. M., The Use of Capacitance Sensors for Phase Percentage Determination in Multiphase Pipelines, *IEEE Transactions on Instrumentation and Measurement*, Vol. 29, 1980, pp. 24-27

[6] Keska J. K., Smith M. D. and Williams B. E., Comparison study of a cluster of four dynamic flow pattern discrimination techniques for multi-phase flow, *Flow Measurement and Instrumentation*, Vol. 10, 1999, pp. 65-77

[7] Strazza D., Demorib M., Ferrari V. and Poesio P., Capacitance sensor for hold-up measurement in high-viscous-oil/conductive-water core-annular flows, *Flow Measurement and Instrumentation*, Vol. 22, 2011, pp. 360-369

[8] Canière H., Bauwens B., T'Joen C. and De Paepe M., Mapping of horizontal refrigerant two-phase flow patterns based on clustering of capacitive sensor signals, *International Journal of Heat and Mass Transfer*, Vol. 53, 2010, pp. 5298-5307

[9] Canière H., Bauwens B., T'Joen C. and De Paepe M., Probabilistic mapping of adiabatic horizontal two-phase flow by capacitance signal feature clustering, *International Journal of Multiphase Flow*, Vol. 35, 2009, pp. 650-660

[10] Canière H., T'Joen C., Willockx A. and De Paepe M., Capacitance signal analysis of horizontal two-phase flow in a small diameter tube, *Experimental Thermal and Fluid Science*, Vol. 32, 2008, pp. 892-904

[11] Canière H., T'Joen C., Willockx A. and De Paepe M., Capacitance sensor design for refrigerant two-phase flow characterization, *Multiphase Flow: The Ultimate Measurement Challenge, Proceedings*, Vol. 914, 2007, pp. 178-183
[12] Thome J. R., Wojtan L. and Ursenbacher T., Measurement of dynamic void fractions in stratified types of flow, *Experimental Thermal and Fluid Science*, Vol. 29, 2005, pp. 383-392
[13] Ghajar A. J. and Woldesemayat M. A., Comparison of void fraction correlations for different flow patterns in horizontal and upward inclined pipes, *International Journal of Multiphase Flow*, Vol. 33, 2007, pp. 347-370
[14] Canière H., Flow Pattern Mapping of Horizontal Evaporating Refrigerant Flow Based on Capacitive Void Fraction Measurements, PhD thesis, Ghent University, Ghent, 2010
[15] Wojtan L., Ursenbacher T. and Thome J. R., Measurement of dynamic void fractions in stratified types of flow, *Experimental Thermal and Fluid Science*, Vol. 29, 2005, pp. 383-392
[16] Cho Y. I. and Greene G. A., Advances in Heat Transfer, Vol. 43, 2011, pp. 175
[17] Wojtan L., Ursenbacher T. and Thome J. R., Investigation of flow boiling in horizontal tubes: Part I - A new diabatic two-phase flow pattern map, *International Journal of Heat and Mass Transfer*, Vol. 48, 2005, pp. 2955-2969
[18] Barbieri P. E. L., Jabardo J. M. S. and Bandarra Filho E. P.,Flow patterns in convective boiling of R-134a in smooth tubes of several diameters *5th European Thermal-Sciences Conference*, The Netherlands, Vol. 2008, pp.
[19] Schubring D. and Shedd T. A., Critical friction factor modeling of horizontal annular base film thickness, *International Journal of Multiphase Flow*, Vol. 35, 2009, pp. 389-397
[20] Oliemans R. V. A., Pots B. F. M. and Trompe N., Modeling of Annular Dispersed 2-Phase Flow in Vertical Pipes, *International Journal of Multiphase Flow*, Vol. 12, 1986, pp. 711-732
[21] Cioncolini A. and Thome J. R., Prediction of the entrained liquid fraction in vertical annular gas–liquid two-phase flow, *International Journal of Multiphase Flow*, Vol. 36, 2010, pp. 293-302
[22] Azzopardi B. J., Measurement of Drop Sizes, *International Journal of Heat and Mass Transfer*, Vol. 22, 1979, pp. 1245-1279
[23] Azzopardi B. J., Drops in annular two-phase flow, *International Journal of Multiphase Flow*, Vol. 23, 1997, pp. 1-53